AD-A088 128 WASHINGTON UNIV SEATTLE SPACE SCIENCES DIV F/G 4/1
2 - 12 MINUTE QUASI-PERIODIC VARIATIONS OF 50 - 1000 KEV TRAPPE--ETC(U)
SEP 75 G K PARSK, C S LIN, J R WINCKLER N00014-67-A-0103-0039

UNCLASSIFIED NL

1 OF 1
AD A
088128

END
DATE
FILMED
9-80
DTIC

PHOTOGRAPH THIS SHEET

AD A088128

DTIC ACCESSION NUMBER

LEVEL: III

INVENTORY

Washington Univ., Seattle

2-12 Minute Quasi-Periodic Variations of 50-1000 keV Trapped Electron Fluxes Detected in the Afternoon Magnetosphere: 2. Theory of Adiabatic Modulations

Contract No. N00014-67-A-103-0039

2 Sept. 1975

DOCUMENT IDENTIFICATION

DISTRIBUTION STATEMENT A

Approved for public release;
Distribution Unlimited

DISTRIBUTION STATEMENT

ACCESSION FOR	
NTIS GRA&I	☒
DTIC TAB	☐
UNANNOUNCED	☐
JUSTIFICATION	
BY Per Ltr. on File	
DISTRIBUTION /	
AVAILABILITY CODES	
DIST	AVAIL AND/OR SPECIAL
A	

DISTRIBUTION STAMP

DTIC
ELECTE
S AUG 22 1980 D
D

DATE ACCESSIONED

DATE RECEIVED IN DTIC

PHOTOGRAPH THIS SHEET AND RETURN TO DTIC-DDA-2

DTIC FORM OCT 79 70A

DOCUMENT PROCESSING SHEET

2 - 12 Minute Quasi-Periodic Variations of 50 - 1000 keV Trapped Electron Fluxes Detected in the Afternoon Magnetosphere:

2. Theory of Adiabatic Modulations

by

C.S. Lin[1] and G.K. Parks[2]
Space Sciences Division of the Geophysics Program
University of Washington, Seattle, WA 98195

and

John R. Winckler
School of Physics and Astronomy
University of Minnesota, Minneapolis, MN 55455

Contract No. [illegible]

ABSTRACT

A simple adiabatic theory of particle modulations is derived. Assuming that the perturbed magnetic field is time dependent but homogenous in space along the dipole direction, an expression for the change of particle fluxes in the equatorial plane is derived in terms of measurable quantities. We show here that the derived expression agrees well with observed characteristics of trapped electron fluxes measured by the University of Minnesota electron spectrometer on the ATS-1. In particular, quasi-periodic modulations of paper 1 are satisfactorily explained.

---

1 Also with the Physics Department

2 Also with the Physics and Atmospheric Sciences Departments

1. Introduction

In Part 1, it was shown that the trapped electron flux variations with time scales of a few minutes are well-organized as a single function of L. We noted in Figure 5 of Part 1, which is reproduced here as Figure 1, that the enhancement of electron fluxes is strongly dependent on the equatorial pitch-angles. In particular, the largest changes are observed near 90° pitch-angles. A conclusion reached by us was that for the most part $\gtrsim$ 50 keV trapped electron fluxes respond adiabatically to local magnetic field changes in the evening magnetosphere.

When the magnetosphere is compressed (inflated) adiabatically, the particle energy and the mirror points will be altered (McIlwain, 1966; Kaufmann, 1974; Murphy et. al., 1975). These changes in particle energy and pitch-angles modulate trapped particle fluxes. If the particle distribution is not uniform in space, a detector fixed in space will observe additional modulations because the detector will be able to scan a range of L-shells (Lezniak and Winckler, 1970; Lin and Parks, 1974). The main purpose of this paper is to show that the features observed by the electron spectrometer reported in Part 1 are consistent with effects that arise when the magnetic field variations are coupled adiabatically to trapped electron fluxes.

Our main interest is to understand quantitatively the variations of the pitch-angle distributions that occur within one oscillation period (see Figure 1). For this study, it will be assumed that the magnetic oscillations have an azimuthal symmetry in the magnetosphere. This assumption is justified if the distance the particles drift in one oscillation period is much less than the size of the oscillation region. Numerically, using the value of the period as 5 minutes and 100 minutes for the drift period, one finds that the oscillation region must be much more extended than about 20° in azimuth. This condition is satisfied because the data strongly suggest that the 2 - 12 minute oscillations are large-scale.

If the magnetic variations have an azimuthal symmetry at all times, it is known that in the absence of steady E-field the drifting particles will always remain on the same L shell (Roederer, 1970). This means that even though the 2-12 minute time scale is shorter than the drift period of the particles, the third invariant will still be conserved during the oscillations. The time scale of interest here is much longer than the cyclotron or the bounce period of these particles. Hence, the first and the second invariants are also conserved. In the quantitative formulation given below, it will be assumed that all of the three invariants are conserved during the oscillations.

The approach taken here is an extension of the work previously published by McIlwain (1966) who studied the adiabatic behavior of trapped equatorially mirroring particles. Conserving all of the three adiabatic invariants, our formulation will include results of particle energy and pitch-angle changes that occur for particles that mirror off the equator. Also, using the Liouville Theorem and a given initial spatial distribution (which is approximated from observations) we will predict the ratios of particle fluxes at two different times at the same geographic location when the magnetic strength changes. The theory is then compared to observations.

The theoretical formulation is presented in Section 2. Application of the theory follows in Section 3.

2. Theoretical Formulation

2.1 A Magnetic Field Model: To describe the adiabatic variations we will assume that the geomagnetic dipole field is perturbed by b(t). b(t) is considered to be only in the z-direction, uniform in space, and time varying.

The expression for the total magnetic field taking into account this perturbation is

$$B(t) = -(2M/r^3)\cos\lambda\hat{r} + (M/r^3)\sin\lambda\hat{\lambda} + b(t)\hat{z} = B_r\hat{r} + B_\lambda\hat{\lambda} \quad (1)$$

M is the dipole moment of the earth and the coordinates $\hat{r}, \hat{\lambda}$, and $\hat{z}$ are the directional unit vectors defined in Figure 2. The equation of a magnetic field line at any time during the perturbation is obtained by integrating $(rd\lambda/B_\lambda) = (dr/B_r)$. Using Equation (1), one obtains

$$r(t) = L\ (1 - br^3/2M)\cos^2\lambda \quad (2)$$

Notice that in the absence of any perturbation (b=0), Equation (2) reduces to the familiar equation for the dipole field line.

Combining Equations (1) and (2) one obtains $B(t,L,\lambda)$, the total magnetic field strength:

$$B(t,L,\lambda) = (M/L^3)(1 + 3\sin\lambda)^{1/2}/\cos^6\lambda + (b/2)(5 + 3\sin^2\lambda)/(1 + 3\sin^2\lambda)^{1/2} \quad (3)$$

When $\lambda=0$, Equation (3) reduces to

$$B(t,L,\lambda=0) = M/L^3 + 5b/2 \quad (4)$$

2.2 Adiabatic Invariants: The expression of the second adiabatic invariant in a time-dependent magnetic field is

$$K(L,\lambda m) = (M/L)^{1/2} \int_0^{\lambda m} \{B(t,L,\lambda m) - B(t,L,\lambda)\}^{1/2}\, ds \quad (5)$$

where λm is the mirror point latitude at time t. This intergral must be computed along the perturbed field line. Using Equation (2), one finds for ds

$$ds = d\lambda L\cos\lambda\ (1 + 3\sin^2\lambda)^{1/2} \left\{ 1 - \frac{\delta\cos^6\lambda\ (1 + 15\sin^2\lambda)}{2(1 + 3\sin^2\lambda)} \right\} \quad (6)$$

Here, δ is defined as bL^3/M.

Let λmo be the particle mirror latitude at $t = t_o$ when there is no magnetic perturbation. Then the second adiabatic invariant $K(L,\lambda m)$ can be Taylor expanded about the unperturbed value $K(L,\lambda mo)$:

$$K(L,\lambda m) = K(L,\lambda mo) + (\lambda m - \lambda mo) \left.\frac{\partial K}{\partial \lambda m}\right|_{\substack{\lambda = \lambda mo \\ \delta = o}} + \delta \left.\frac{\partial K}{\partial \delta}\right|_{\substack{\lambda m = \lambda mo \\ \delta = o}} \quad . \; . \; . \; . \; (7)$$

The conservation of the second invariant means that $K(L,\lambda m) = K(L,\lambda mo)$

From Equation (7), λm and λmo are related by

$$\lambda m = \lambda mo - \delta(\partial K/\partial \delta)/(\partial K/\partial \lambda m) \quad . \; (8)$$

It can be shown that $\partial K/\partial \delta < o$. Hence, $\lambda m > \lambda mo$ when $\delta > o$. This means that the particle mirror latitude is lowered toward the earth when the magnetosphere is compressed.

$(\lambda m-\lambda mo)/\delta$ is plotted in Figure 3 as a function of the equatorial pitch-angle α_o. For practical purpose, the ratio $(\lambda m-\lambda mo)/\delta$ can be expressed with an error of less than 1% by the following

$$(\lambda m-\lambda mo)/\delta = 0.30\mathrm{Sin}4\lambda m + 0.11\mathrm{Sin}2\lambda m \quad . \; . \; . \; . \; . \; . \; . \; . \; . \; . \; . \; . \; . \; . \; . \; . \; . \; . \; (9)$$

Now we compute the corresponding change of energy during the adiabatic compression using the first adiabatic invariant. Let E_o be the particle energy at t_o and E be the energy at time t. Then it follows that

$$E/E_o = B(t,L,\lambda m)/Bt_o, L,\lambda mo) = 1 + (1/B)(\partial B/\partial \lambda m)(\lambda m - \lambda mo)$$
$$+ (\delta/B)(\partial B/\partial \delta) \quad . \; . \; . \; . \; . \; . \; . \; . \; . \; . \; . \; . \; . \; . \; . \; (10)$$

The derivatives are to be evaluated at $\lambda m = \lambda mo$ and $\delta = 0$. It can be shown using Equation (3) that

$$\left(\frac{1}{B}\right)\left(\frac{\partial B}{\partial \lambda m}\right) = (3\mathrm{Sin}\lambda m/\cos\lambda m)\,\frac{(3 + 5\,\mathrm{Sin}^2\lambda m)}{(1 + 3\,\mathrm{Sin}^2\lambda m)} \quad . \; . \; . \; . \; . \; . \; . \; . \; . \; . \; . \; . \; . \; . \; (11)$$

and

$$(\frac{1}{B})(\frac{\partial B}{\partial \delta}) = \cos^6\lambda m \frac{(5 + 3\sin^2\lambda m)}{2(1 + 3\sin^2\lambda m)} \quad (12)$$

Equation (10) can be rewritten as

$$E/Eo = 1 + \delta\left[G(\lambda mo) + H(\lambda mo)\right] \quad (13)$$

where $G(\lambda m)$ and $H(\lambda m)$ are defined as

$$G(\lambda m) = (1/B)(\frac{\partial B}{\partial \lambda m})(\lambda m - \lambda mo)/\delta \quad (14)$$

and

$$H(\lambda m) = \frac{1}{B}\frac{\partial B}{\partial \delta} \quad (15)$$

Figure 4 shows the plot of the functions $G(\lambda m)$ and $H(\lambda m)$. Note that $H(\lambda m)$ is larger at large pitch-angles while $G(\lambda m)$ is larger at small pitch-angles. Physically, $G(\lambda m)$ is related to the change of the mirror points and therefore is due to Fermi acceleration. $H(\lambda m)$ is related to compressional effects and therefore is due to batatron acceleration. Note that at 30^o pitch-angle, the contribution from Fermi and betatron actions are equal.

<u>2.3 Particle Flux Modulation</u>: Let $J(E,\alpha, t,L)$ be the differential particle flux at energy E and pitch-angle α at time t at the magnetic coordinate L. L is related to the position r through Equation (2). To understand the particle flux modulation due to adiabatic effects, let γ be the ratio of particle fluxes at the energy E and pitch-angle α measured at the times t and t_o at the coordinates L and L_o:

$$\gamma = J(E,\alpha,t,L)/J(E,\alpha,t_o,L_o) \quad (16)$$

L and L_o are the magnetic coordinates at the position r at times t and t_o. t_o cooresponds to the time when the magnetic perturbation is zero. Since our intention is to understand observational features in the equatorial plane, in the subsequent computations we will set $\lambda=0$. From Equation (2), one then notes that $L_o = r$ and $L = r/(1 - br^3/2M)$.

Using Liouville's theorem and the fact that particles in our model remain on the same L shell during the perturbation, we can conclude that

$$J(E,\alpha,t,L) = (E/E_o)\ J(E_o,\alpha_o,t_o,L) \quad \text{(17)}$$

The relation between E and E_o is obtained from Equation (13). The relation between (α) and (α_o) can be derived from the first aidabatic invariant. Then,

$$\sin^2\alpha/\sin^2\alpha_o = (E_o/E)B(t,L,\lambda = 0)/B(t_o,L,\lambda = 0) \quad \text{(18)}$$

Here $B(t_o,L,\lambda = 0) = M/L^3$ and using Equation (4), one finds that $B(t,L,\lambda = 0) = B(t_o,L,\lambda = 0) + 2.5b$.

Let us now assume that $J(E,\alpha,t_o,L)$ can be represented as

$$J(E,\alpha,t_o,L) = CB^a(t_o,L)E^{-n}\sin^m\alpha \quad \text{(19)}$$

Then, substituting Equations (17), (18), and (19) into Equation (16), one obtains

$$\gamma = (E_o/E)^{-1-n-m/2}\ B(t_o,L_o)^{-a}B(t_o,L)^{a-m/2}B(t,L)^{-m/2} \quad \text{(20)}$$

From Equation (1), note that $B(t,L,\lambda = 0) = B(t_o,L_o,\lambda = 0) + b(t)$.

We now use Equation (13) and the relationship between B(t,L) and $B(t_o,L_o)$ and $B(t_o,L)$ to derive

$$\gamma = 1 + \delta\left[(1 + n + m/2)(G(\lambda mo) + H(\lambda mo)) - 1.5a - 1.25m\right] \quad \text{(21)}$$

Note that Equation (21) reduces to Equation (15) of McIlwain (1966) for $\lambda mo = 0$ and $m = 0$. All quantities in Equation (21) are measurable experimentally.

3. Application of the Adiabatic Theory

We wish to compare Equation (21) to data obtained at synchronous altitudes. Using Figure 4 of Paper 1, we obtain the value for "a" to be ~ 4.5. This value was obtained for flux variations that occurred in the interval of time around 0100 - 0200 U.T. In Figure 5, we have plotted $(\Delta J/J)/(\Delta B/B) = (\delta - 1)/\delta$ as a function of the equatorial pitch-angles of the particles. The three points shown in the pitch-angle range about 70^{o} - 90^{o} are obtained from the ATS-1 electron data and they represent values of particles whose energy is greater than 50 keV. These points were obtained for the variations that occurred in the UT time interval 0100 - 0200. Here ΔJ represents the flux changes that occurred from minimum to maximum during the changes of the local magnetic field intensity ΔB. The values shown are averages of seven modulation events that occurred in this time interval, (Figure 1 shows a typical example).

The experimentally computed values have been compared against the theoretical curves obtained from Equation (21). Since Figure 1 suggests that m is negative, we have used $m = -1$ in our computation. With this value of m, we find that the expeimental values agree best with the theory for n between 3 and 4 (see Figure 5).

The ATS-1 electron spectrometer was not designed to obtain accurate energy spectral estimates since the energy windows are wide. However, the energy spectral index predicted by the adiabatic theory suggests that during the modulation events the index was around 3 and 4. It is worthy of note that such index values for trapped electron fluxes are quite reasonable on the basis of other observations (McIlwain, 1966; Lezniak and Winckler, 1970; Pizzela and Frank, 1971).

The ATS-1 only provided data in the large pitch-angle interval. While the theory and the data agree well here, we do not have at this time data at small pitch-angles to verify whether the theory is valid there. An important point to note is that below about 40° pitch-angle, $(\Delta J/J)/(\Delta B/B)$ becomes negative (Figure 5). This means that the particle fluxes at small pitch-angles decrease when the magnetosphere is compressed, an opposite behavior to the particles at large pitch-angles. Physically, this effect can be understood by noting that the particle flux changes are due to the combined effects of betatron and Fermi accelerations and L-shell modulation.

4. Discussion

In our formulation of the adiabatic modulation theory, recall that we considered that the perturbed magnetic field is only in the dipole direction. In reality, however, perturbations are also observed in the transverse directions (Barfield and McPherron, 1972; Lin and Parks, 1974). The fact that the limited theory still agrees well with the observations suggests that the effects from transverse perturbations are small. Qualitatively, this can be understood by noting that in the expression of the first invariant $\mu = E/\{(B_o + b_{\parallel})^2 + b_{\perp}^2\}^{1/2}$ the energy change is proportional to $b_{\parallel}/B_o$ and $b_{\perp}^2/B_o^2$. Evidently, the second order effects are negligible.

Additionally, the model presented here did not include effects of convection and radial diffusion in computing the particle flux modulations. While this omission is justified for studying particle modulations of a few minutes period, these effects must be included if the time scales involved are comparable to convective and diffusive times.

In spite of the simplicity of our model, the theory has provided a means for separating the adiabatic and non-adiabatic effects in the data, making it possible to study more quantitatively the contributions of non-adiabatic processes. We are currently in the process of removing the adiabatic effects in particle acceleration events to study in more detail the non-adiabatic contributions.

ACKNOWLEDGEMENT

The research at the University of Washington is supported in part through grants received from the National Aeronautics and Space Administration NGR 48-002-154, the National Science Foundation Grant DES 74-02762 A01, and the Office of Naval Research Contract N00014-67-A-0103-0039. The ATS-1 program at the University of Minnesota was supported by the National Aeronautics and Space Administration Contract NASS-9542.

REFERENCES

McIlwain, C.E., Ring current effects of trapped particles, J. Geophys. Res., 71, 3623, 1966.

Lin, C.S. and G.K. Parks, Further characteristics of the evening energetic electron decreases during substorms, J. Geophys. Res., 79, 3201, 1974.

Lezniak, T.W. and J.R. Winckler, Experimental study of the magnetosphere motions and the acceleration of energetic electrons during substorms, J. Geophys. Res., 75, 7075, 1970.

Kaufmann, R.L., Electron acceleration during tail collapse, J. Geophys. Res., 79, 549, 1974.

Murphy, C.H., C.S. Wang and J.S. Kim, Mirror height lowering of trapped electrons by an inductive electric field, J. Geophys. Res., 80, 1346, 1975.

Roederer, J., Dynamics of geomagnetically trapped radiation, Springer-Verlag Berlin, Heidelberg, 1970.

FIGURE CAPTIONS

Figure 1: Behavior of pitch-angle distribution during adiabatic oscillations. Large enhancements in fluxes are observed at high pitch-angles.

Figure 2: Coordinate system used for the geomagnetic field perturbation.

Figure 3: Fractional change of the mirror latitude normalized to the fractional change in the magnetic field strength as a function of the mirror latitude and equatorial pitch-angle. Corresponding equatorial pitch-angle scale is shown in the top scale.

Figure 4: Fractional change of the particle energy normalized to the fractional change of the magnetic field intensity due to betatron and Fermi acceleration. Note that equal effects are observed at about 30° equatorial pitch-angle.

Figure 5: Fractional change of fluxes predicted normalized to the fractional change of the magnetic field intensity as a function of the equatorial pitch-angle. The solid curves are derived assuming a form of the distribution shown. "a" is a measure of the gradient and is derived from observations. Observed data points from June 26, 1967 events are shown to agree with the theoretical predications with the parameters indicated in the solid curves.

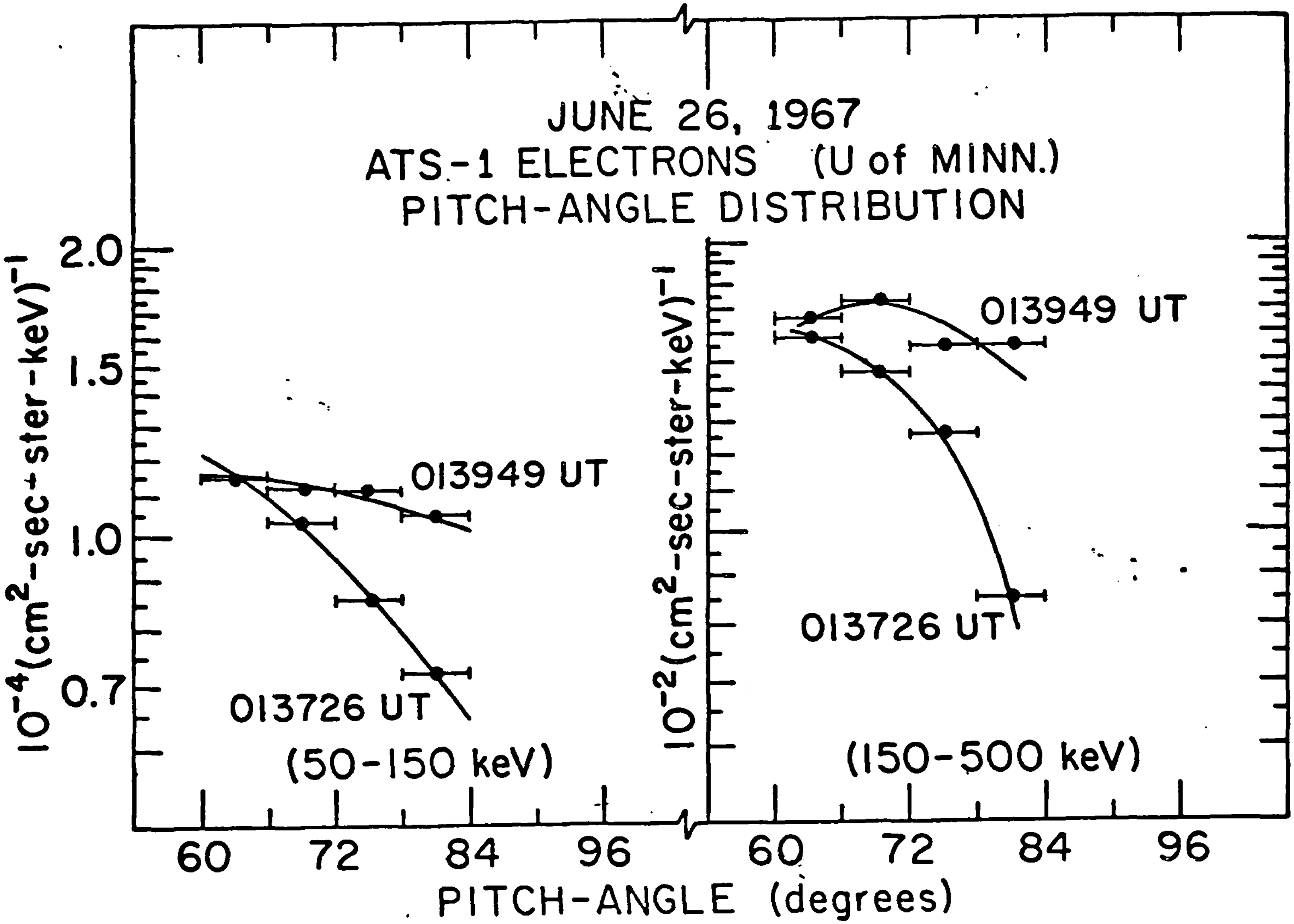

JUNE 26, 1967
ATS-1 ELECTRONS (U of MINN.)
PITCH-ANGLE DISTRIBUTION
$10^{-4}(cm^2\text{-sec-ster-keV})^{-1}$
2.0
1.5
1.0
0.7
013949 UT
013726 UT
(50-150 keV)
$10^{-2}(cm^2\text{-sec-ster-keV})^{-1}$
013949 UT
013726 UT
(150-500 keV)
60
72
84
96
60
72
84
96
PITCH-ANGLE (degrees)

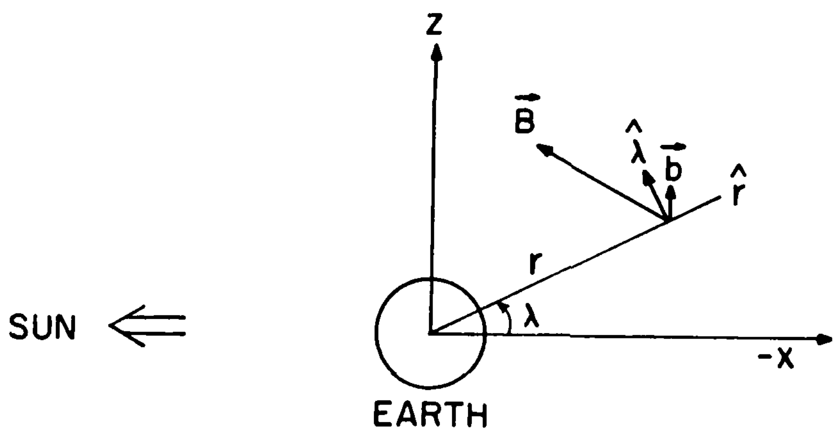

Z
$\vec{B}$
$\hat{\lambda}$
$\vec{b}$
$\hat{r}$
r
SUN
λ
-X
EARTH

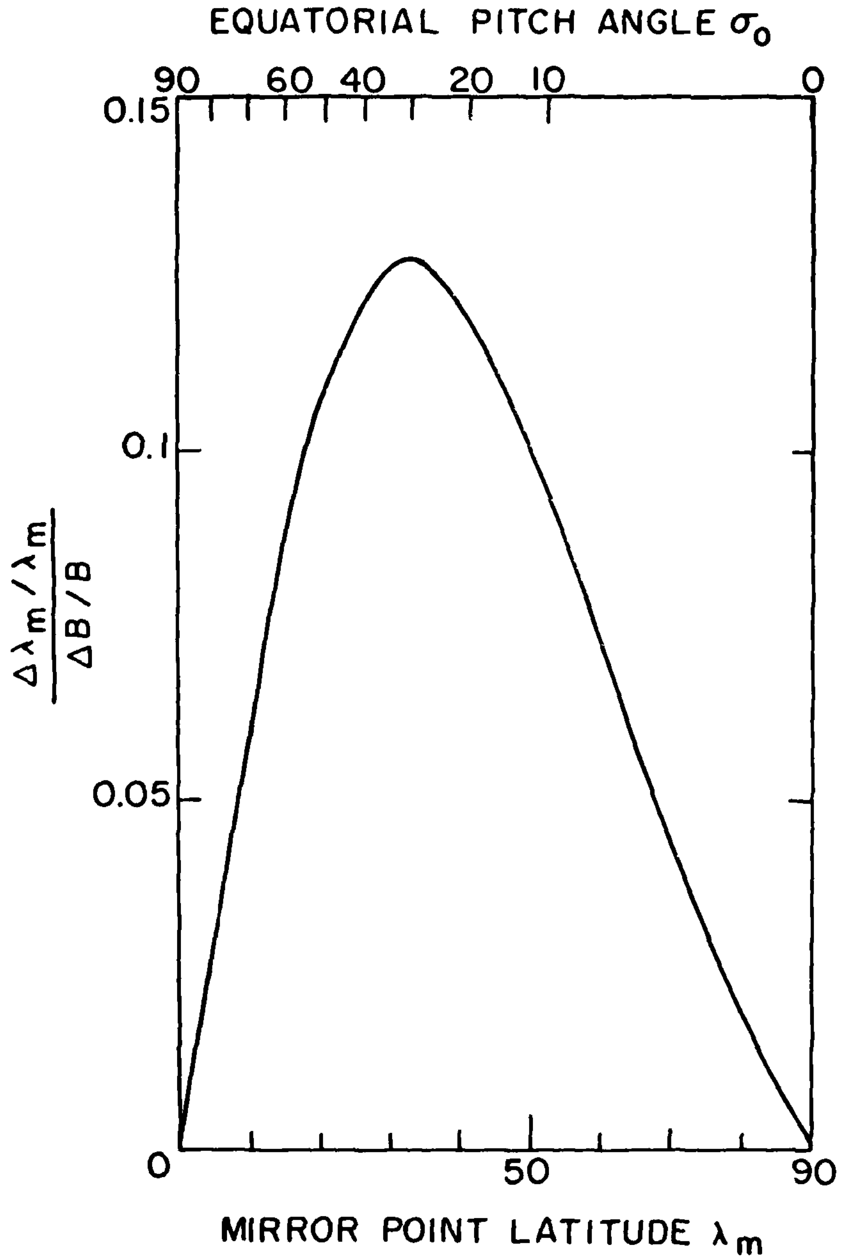
EQUATORIAL PITCH ANGLE σ_0
90
60
40
20
10
0
0.15
0.1
0.05
0
$\frac{\Delta\lambda_m/\lambda_m}{\Delta B/B}$
50
90
MIRROR POINT LATITUDE λ_m

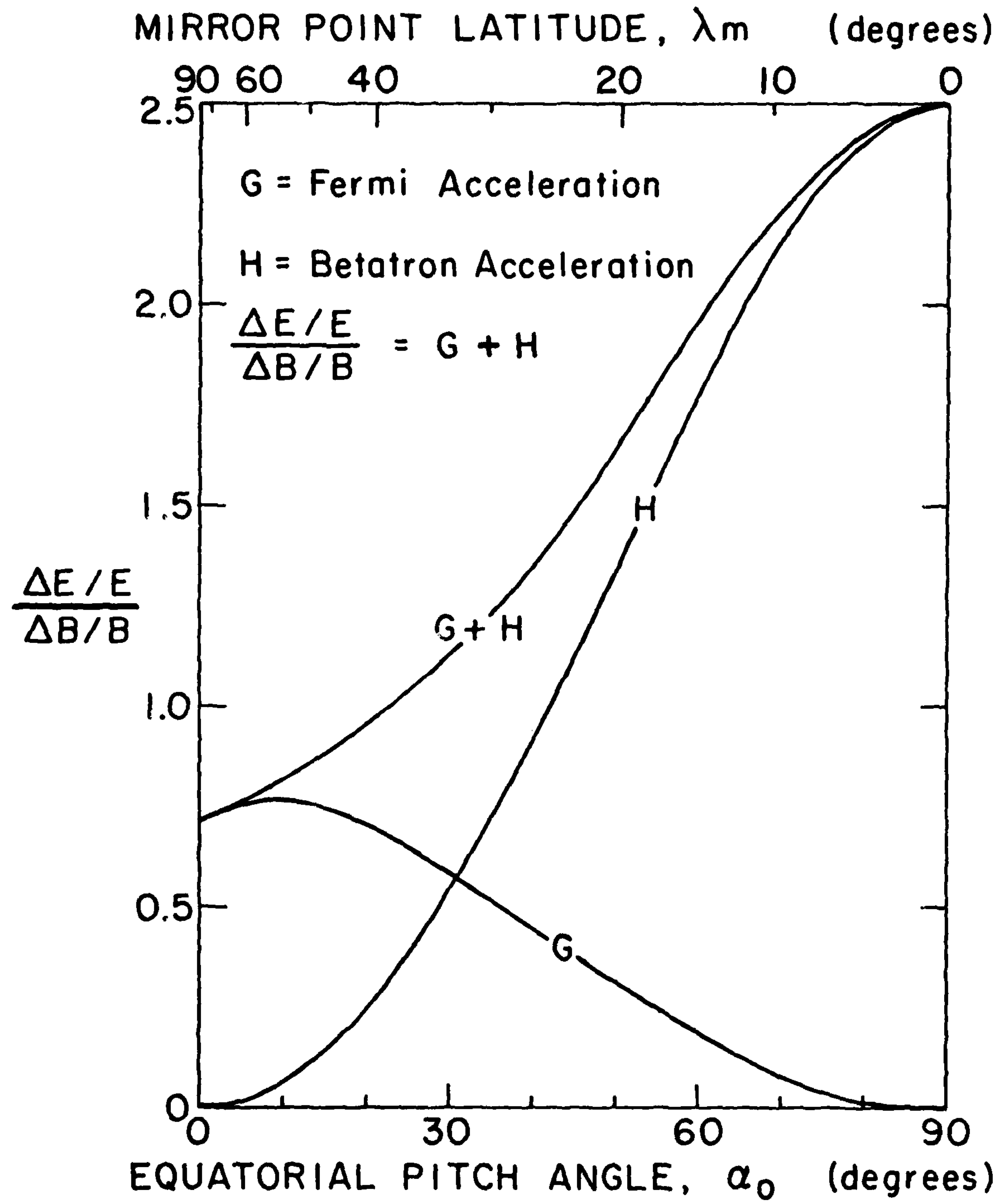

MIRROR POINT LATITUDE, λm (degrees)
90 60 40 20 10 0
2.5
2.0
1.5
1.0
0.5
0
G = Fermi Acceleration
H = Betatron Acceleration
$\frac{\Delta E/E}{\Delta B/B}$ = G + H
$\frac{\Delta E/E}{\Delta B/B}$
G+H
H
G
0 30 60 90
EQUATORIAL PITCH ANGLE, α_0 (degrees)

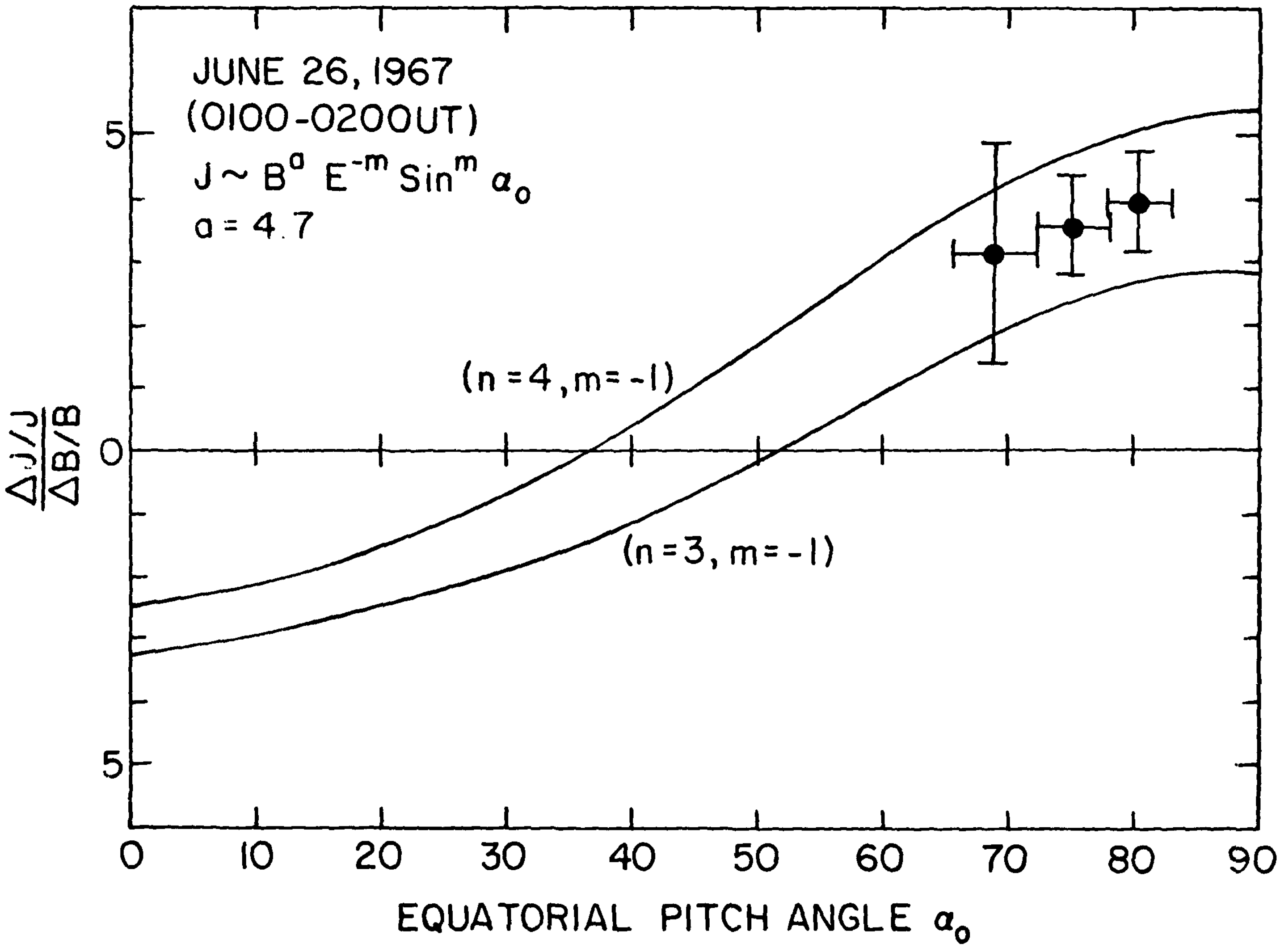
JUNE 26, 1967
(0100-0200UT)
$J \sim B^a E^{-m} \mathrm{Sin}^m \alpha_0$
a = 4.7
(n = 4, m = -1)
(n = 3, m = -1)
$\frac{\Delta J/J}{\Delta B/B}$
5
0
5
0
10
20
30
40
50
60
70
80
90
EQUATORIAL PITCH ANGLE α_0